*Journal of Sound and Vibration* (2001) **244**(5), 871–881
doi:10.1006/jsvi.2000.3520, available online at http://www.idealibrary.com on IDEAL®

# DEVELOPMENT OF OPTIMALLY DISORDERED CRITICAL RANDOM EXCITATION

S. KHAJEHPOUR

*Department of Civil Engineering, University of Waterloo, Waterloo, Ontario, Canada*

AND

A. SARKAR

*Department of Civil Engineering, The Johns Hopkins University*, 3400 *N. Charles Street, Baltimore, MD* 21218, *U.S.A. E-mail: asarkar@mars.ce.jhu.edu*

(*Received* 18 *January* 2000, *and in final form* 12 *December* 2000)

The problem of determining the critical power spectral density (PSD) function of a partially specified stationary Gaussian load process which maximizes the response of a linear system has been considered. The partial specification of the load is given only in terms of its total average energy. The critical input PSD turns out to be highly narrow banded which fails to capture the erratic nature of the excitation. Consequently, the trade-off curve between the maximum linear system response and the disorder in the input process, quantified in terms of its entropy rate, has been generated. The Pareto optimization theory is used to tackle the conflicting objectives of simultaneous maximization of the system response and the input entropy rate. Consequently, the non-linear multi-objective optimization has been carried out using a Multi-criteria Genetic Algorithm scheme. An illustrative example of determining the critical input of an axially vibrating rod excited by a partially specified stationary Gaussian load process has been considered.

© 2001 Academic Press

## 1. INTRODUCTION

The reliable and complete description of random excitation necessary for the response analysis of engineering structures are difficult to obtain on numerous occasions. For example, the description of seismic excitations is fraught with uncertainties due to various factors such as the nature and number of earthquakes, its travel path, the local geological effects and scarcity of recorded data. The method of critical excitation is primarily developed to deal with the response analysis of engineering systems to incompletely specified inputs. The method is based on the philosophy that the random input can only be specified partially with confidence. The missing information about the input required for the complete response analysis is determined such that the damage to a given system is maximized.

The determination of critical excitation constitutes an inverse problem of engineering system analysis. Early studies in the context of electrical circuit had been carried out by Tufts and Shnidman [1]; and Papoulis [2, 3] who determined the critical input wave forms with the constraints on the total energy and peak values which maximizes the linear system response. In the context of earthquake engineering, the problem of obtaining the critical seismic input was initiated by Drenick [4]. The subsequent research was primarily focussed to evolve the same concept (e.g. references [5, 6]). The aforementioned studies were primarily carried out in

0022-460X/01/300871 + 11 $35.00/0 © 2001 Academic Press

the deterministic framework. The problem of characterizing the critical excitation in terms of a Gaussian random process has been proposed by Iyengar and Manohar [7, 8]. The list of studies conducted in the context of determining the critical excitation cited above is by no means complete. To place the scope of this paper in proper perspective, only a few papers from the vast number of the relevant literature is mentioned above. The reader may further refer to Sarkar [9] for an elaborate review of previous works conducted in this area.

From the previous study carried out in the context of earthquake excitation [9, 10], the worst input turned out to be highly narrow-banded when the available information of the excitation is given in terms of its total average energy and the mean zero-crossing rate, as to be expected intuitively. The narrow-banded nature of the input actually represents the resonant phenomenon and thus, fails to account for the random nature of the input. To circumvent this problem, the entropy rate of the input is proposed as a measure of disorder to the critical excitation which captures its erratic nature. Consequently, the critical excitation is redefined as the input which simultaneously maximizes the system response and the input entropy rate. It also emerges that the maximization of the input entropy rate criteria alone demands the response to be highly broad-banded. Thus, the response maximization criterion is in direct conflict with the requirement of the input entropy rate maximization. This constitutes a typical non-linear multi-criteria optimization problem with conflicting objectives. There are two general approaches to solve such a problem, namely, the preference and non-preference methods. The preference method makes use of explicit information about the relative importance of different objective criteria in order to identify a best overall solution. This approach was adopted in the previous work [9, 10] using the calculus of variation and linear programming methods to solve the problem indirectly. In this paper, the non-preference method often referred to as Pareto optimization technique has been used to solve the problem directly.

In Pareto optimization procedures, no assumption about the relative importance of the different objective criteria is made *a priori*. But instead, it identifies a field of solutions that are all considered to be of equal rank from the perspective of all objective criteria. Consequently, it is then left to the designer to choose a solution from these equal-rank solutions, based on knowledge of the trade-off between performance in different objective functions. The decision about choosing a critical input can be made based on various criteria such as the risk level acceptable to the designer, the entropy rate associated with the input obtained from recorded data, etc.

Furthermore, a powerful numerical optimization procedure based on Multi-criteria Genetic Algorithm (MGA) has been used to deal with the non-linear optimization problem. The method has been applied to develop the critical excitation of a linear multi-degree-of-freedom system based on various response maximization criteria with the constraint on the total energy of the input.

## 2. MATHEMATICAL FORMULATION

### 2.1. INPUT SPECIFICATION

In the present study, the excitation driving the linear system is modelled as a stationary Gaussian random process with unknown PSD $S(\omega)$. The total average energy $E$ is assumed to be known and given by

$$E = \int_{\omega_1}^{\omega} S(\omega)\,\mathrm{d}\omega, \tag{1}$$

where $(\omega_1, \omega_2)$ is the bandwidth of the excitation, also assumed to be known.

### 2.2. INPUT ENTROPY RATE

In tackling the problem of critical excitation, one essentially deals with an incompletely specified probability space. In fact, a similar situation arises in various branches of engineering. The principal of maximum entropy has been developed to handle these problems [11, 12].

For a continuously distributed random variables $X$, the expression for entropy is

$$H_x = \int_{-\infty}^{\infty} p(x) \ln p(x) \, \mathrm{d}x, \tag{2}$$

where $p(x)$ is the probability density function (pdf) of $X$. According to the maximum entropy principle, the most uncertain pdf of $X$ can be found by maximizing $H_x$ subject to constraints reflecting the properties of $X$. For example, the maximum entropy probability distribution of a continuously distributed random variable with known range $(x_1, x_2)$ is a uniform distribution between $(x_1, x_2)$. The principle of maximum entropy [11] has been extended to the random process where one has to consider the entropy rate of the signal. For an incompletely specified band-limited stationary random process $w(t)$, the unspecified parameter of the process can be determined by maximizing the entropy rate of the process,

$$\bar{H}_W = \lim_{n \to \infty} \frac{1}{n} \int_{-\infty}^{\infty} p(w) \ln p(w) \, \mathrm{d}w, \tag{3}$$

where $p(w)$ is the $n$-dimensional joint pdf of the random process $w(t)$ sampled at $t_1, \ldots, t_n$. For a stationary band-limited Gaussian random process, the entropy rate can be expressed in terms of its PSD function $S(\omega)$ as in reference [11],

$$\bar{H}_W = \ln \sqrt{2\pi e} + \frac{1}{2(\omega_1 - \omega_2)} \int_{\omega_1}^{\omega_2} \ln S(\omega) \, \mathrm{d}\omega. \tag{4}$$

It can easily be shown that the maximum entropy power spectral density of a Gaussian random process with given variance $E = \int_{\omega_1}^{\omega_2} S(\omega) \, \mathrm{d}\omega$ is a band-limited white noise as given by

$$S(\omega) = \frac{E}{(\omega_1 - \omega_2)}. \tag{5}$$

### 2.3. RESPONSE SPECIFICATION

From the linear random vibration analysis, the stationary response variance of a linear system at any point $x$, driven by a stationary random excitation, can be expressed as in reference [13]:

$$\sigma^2(x) = \int_{\omega_1}^{\omega_2} H(\omega, x) S(\omega) \, \mathrm{d}\omega, \tag{6}$$

where $H(\omega, x)$ is the frequency response function of the linear system.

The expression for the mean response zero crossing rate is given by [13]

$$v(0) = \frac{1}{\pi} \frac{[\int_{\omega_1}^{\omega_2} \omega^2 H(\omega, x) S(\omega)\, \mathrm{d}\omega]^{1/2}}{[\int_{\omega_1}^{\omega_2} H(\omega, x) S(\omega)\, \mathrm{d}\omega]^{1/2}}. \tag{7}$$

The aforementioned response quantities are indicators of two major failure criteria of the system. The maximization of the response variance in fact maximizes the system failure due to the extreme events. On the other hand, the maximization of the mean zero-crossing rate maximizes the fatigue failure of the system.

### 2.4. OPTIMIZATION PROBLEM

In this section, the optimization problem of maximizing the response quantities as well as maximizing the input entropy rate is formulated.

We discretize the input PSD function $S(\omega)$ by the expression

$$S(\omega) = \sum_{n=1}^{N} a_n \delta(\omega - \omega_n), \tag{8}$$

where $\delta(\cdot)$ is the Dirac-delta function and $a_n$, $n = 1, \ldots, N$ are the optimization variables which determine the shape of critical input PSD function $S(\omega)$.

Consequently, the multi-criteria optimization problem, involving the two aforementioned response quantities and the input entropy rate, is stated below.

#### 2.4.1. *Case-A*

Firstly, we consider the problem of maximizing the response variance $\sigma^2$ and the term involving input PSD in the expression of its entropy rate in equation (4), namely $\tilde{H}_W = \int_{\omega_2}^{\omega_2} \ln S(\omega)\, \mathrm{d}\omega$. Using the discretized form of the input PSD in equation (8), the optimization problem of maximizing $\sigma^2$ and $\tilde{H}_W$ can be posed as

$$\max \sigma^2 = \sum_{n=1}^{N} a_n H(\omega_n, x), \qquad \max \tilde{H}_W = \mathrm{d}\omega \sum_{n=1}^{N} \ln\left(\frac{a_n}{\mathrm{d}\omega}\right), \tag{9, 10}$$

subject to

$$\sum_{n=1}^{N} a_n = E. \tag{11}$$

#### 2.4.2. *Case-B*

Next we consider the problem of optimizing the mean zero-crossing rate $v(0)$ in equation (7) and the scaled input entropy rate $\tilde{H}_W$. Using the discretized form of the input PSD given in equation (8), this problem can again be expressed as

$$\max \pi v(0) = \frac{[\sum_{n=1}^{N} \omega_n^2 H(\omega_n, x) a_n]^{1/2}}{[\sum_{n=1}^{N} H(\omega_n, x) a_n]^{1/2}}, \qquad \max \tilde{H}_W = \mathrm{d}\omega \sum_{n=1}^{N} \ln\left(\frac{a_n}{\mathrm{d}\omega}\right), \tag{12, 13}$$

subject to

$$\sum_{n=1}^{N} a_n = E. \tag{14}$$

It should be noted that the maximization of $\sigma^2$ under the constraint of $E$ constitutes a standard problem of linear programming. The result is shown to be a Dirac-delta function representing a harmonic excitation indicating the resonant phenomenon [9, 10]. On the other hand, the maximization of $\tilde{H}_W$ under the constraint of $E$ can be performed using calculus of variation and is given by a band-limited noise as discussed before. Thus, the maximization of $\sigma^2$ demands the input to be highly narrow-banded whereas the maximization of $\tilde{H}_W$ requires the input to be highly broad-banded. One can easily observe that the two objective functions are directly in conflict. The maximization of the mean zero-crossing rate $v(0)$ under the constraint of $E$ is highly non-linear and requires the solution of the non-linear simultaneous equations, which does not permit simple solutions, unlike the first case discussed above.

### 2.5. PARETO OPTIMIZATION PROCEDURE

In numerous engineering applications, the designer has to consider several compromise designs by trading off the performances between various objectives with conflicting requirements. The method of Pareto optimization is specifically suitable to tackle such problems. This method makes no assumption about the relative importance of different objective criteria, but rather identifies a field of solutions that are all considered to be of equal rank in the sense that no particular solution is better than any other with respect to all objective criteria. It is then left to the designer to choose a solution from the pool of equal ranking solutions, based on the knowledge of the trade-off between performances of different objective criteria (Pareto design). The concept of multi-criteria Pareto optimization is briefly explained below.

The multi-criteria optimization problem can be stated as follows:

$$\text{maximize} \quad \mathbf{f}(\mathbf{x}) = [f_1(\mathbf{x}), f_2(\mathbf{x}), \ldots, f_Q(\mathbf{x})]^{\mathrm{T}}, \tag{15}$$

$$\text{subject to} \quad \mathbf{g}(\mathbf{x}) \leqslant 0, \mathbf{h}(\mathbf{x}) = 0, \tag{16}$$

where $\mathbf{x} = [x_1, x_2, \ldots, x_n]^{\mathrm{T}}$ is the vector of $n$ design variables, $\mathbf{f}(\mathbf{x})$ is the vector of $i = 1, 2, \ldots, Q$ objective functions $f_i(\mathbf{x})$ that are each to be maximized for the design subject to the equality and non-equality constraints: $\mathbf{h}(\mathbf{x}) = 0$ and $\mathbf{g}(\mathbf{x}) \leqslant 0$. A design $\mathbf{x}^0$ is Pareto optimal for the problem, if there exists no other design $\mathbf{x}$ for which $f_i(\mathbf{x}) \geqslant f_i(\mathbf{x}^0)$ for $i = 1, 2, \ldots, Q$ with $f_i(\mathbf{x}) > f_i(\mathbf{x}^0)$ for at least one objective criterion. In other words, the design $\mathbf{x}^0$ is Pareto optimal if there exists no other feasible design $\mathbf{x}$ which dominates it for all objective criteria. The Pareto-optimal design set is the set of designs distributed along the Pareto-optimal curve/surface defining the trade-off between the different objective criteria. From a population of $N$ designs, the number of $P$ designs belonging to the Pareto-optimal design set can be anywhere in the range of $1 \leqslant P \leqslant N$.

For a more elaborate description of the Pareto optimization procedure, the reader can refer to Pareto [14] and Koski [15].

### 2.6. MULTI-CRITERIA GENETIC ALGORITHM (MGA) IMPLEMENTATION

The multicriteria optimization stated above entails finding the set of solutions defining the trade-off (Pareto) curves spanning between the different competing criteria. The aforementioned optimization procedure can be conveniently performed using MGA as it always works with a population of solutions rather than one solution at a time and is

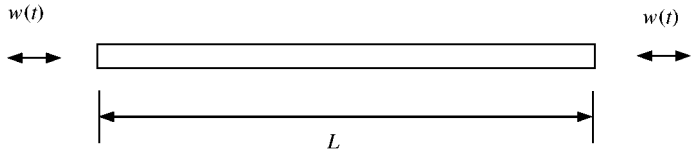


Figure 1. Axially vibrating rod.

particularly suitable for multi-objective optimization. The reader may refer to Goldberg [16] for the comprehensive details on GA. The fitness function used here is based on a distance metric related to the Pareto optimal set. Consequently, the chance of survival of a design in the next generation depends on its relative distance from the current Pareto set determined as

$$D(\mathbf{x}) = \min \sqrt{\left(\frac{f_{1n}^p - f_1(\mathbf{x})}{f_{1n}^p}\right)^2 + \left(\frac{f_{2n}^p - f_2(\mathbf{x})}{f_{2n}^p}\right)^2}, \quad n = 1, \ldots, n_p, \tag{17}$$

where $n_p$ is the number of existing Pareto design, $f_{1n}^p$, $f_{2n}^p$ the objective value for the Pareto design $n$ and $f_1$, $f_2$ the objective value of design $\mathbf{x}$. It should be noted that $f_1$ and $f_2$ relate $\sigma^2$ and $\tilde{H}_W$ in equations (9) and (10); and $\pi v(0)$ and $\tilde{H}_W$ in equations (12) and (13). The elements of the design variable vector $\mathbf{x}$ correspond to $a_n$, $i = 1, \ldots, N$ in equation (8).

The relative distance between design $\mathbf{x}$ and the Pareto set is taken to be the distance to the nearest Pareto design. Obviously, the distance of each Pareto design to the Pareto set is zero. Consequently, the fitness $\mathbf{F}(\mathbf{x})$ of each design $\mathbf{x}$ is found as

$$\mathbf{F}(\mathbf{x}) = F_{max} - D(\mathbf{x}), \tag{18}$$

where $F_{max}$ is a large number, chosen to be greater than the maximum of $D(\mathbf{x})$ for all the design vector $\mathbf{x}$. The members of the next generation are chosen based on this fitness criterion. The genetic operators of cross-over and mutation for the optimization are the same as the conventional GA scheme [16]. The elitist strategy ensures the survival of the previous Pareto set into the next generation. After these operations, a new Pareto set is found. The procedure is repeated until convergence is achieved when there is no change in the Pareto optimal set for a preassigned number of consecutive generations, at which point the MGA run is terminated. As for GA, multiple runs are conducted and the overall Pareto optimal set is taken as the combined set of Pareto optimal design found from all runs.

## 3. NUMERICAL RESULTS

As a numerical example of the formulation, the axial vibration of a rod shown in Figure 1 excited by its support motion $w(t)$ has been studied. The following properties of the rod has been considered for the numerical investigation: mass/unit length $m = 100$ kg/m; axial stiffness $EA = 4{\cdot}05 \times 10^5$ N; the viscous damping/unit length $C_1 = 5$ Ns/m$^2$; the strain rate dependent damping $C_2 = 1000$ N s. The undamped natural frequencies of an axially vibrating rod are equally spaced in the frequency axis. The transfer function of the system can be shown to be given by

$$H(\omega, x) = \left| \left( \frac{1 - \cos kL}{\sin kL} \right) \sin kx + \cos kx \right|^2, \tag{19}$$

where $k = \sqrt{(\omega^2 m - \mathrm{i}\omega c_1)/(EA + \mathrm{i}\omega c_2)}$.

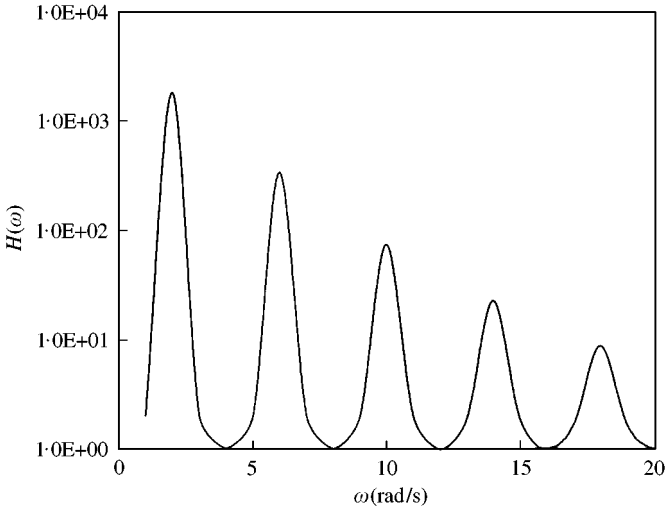


Figure 2. The system transfer function.

The average energy of the excitation $w(t)$ is $E$ and arbitrarily taken to be 4·0 in the numerical study. The band limit of the excitation $(\omega_1, \omega_2)$ is assumed to be (1, 20) rad/s.

Figure 2 shows the system transfer function at $x = L/2$. It should be noted that the natural frequencies of the rod excited by its support motion are at 2, 6, 10, 14 and 18 rad/s. These are in fact the first, third, fifth, seventh and ninth natural frequencies of the rod.

In the numerical investigations, the following parameters are taken: the number of optimization variables is $N = 20$; each $a_n$ is discretized by 127 points between 0·0001 and 4; the number of population for each GA run is 1000, the mutation rate is taken to be 0·05. Figure 3(a) and (b) show the critical PSD functions; and the trade-off curve of the response variance and the entropy rate of the excitation. In Figure 3(a), the critical PSD functions which maximize the response variance $\sigma^2$ are shown for various levels of entropy rate $\tilde{H}_W$, as marked in the trade-off curve in Figure 3(b). In other words, these PSD functions also represent the excitations which maximize the input entropy rate for various levels of response variances. In Figure 3(b), case 1 shows the result when the maximization of the response variance $\sigma^2$ receives the highest priority resulting in a nearly deterministic harmonic input indicating a resonant phenomenon. The same result is obtained in the previous studies [9, 10] using the linear programming method. Cases 2 and 3 show the critical PSD functions for the increasing level of input entropy rate $\tilde{H}_W$ as indicated in the trade-off curve in Figure 3(a). It can be observed from Figure 3(a) that the critical inputs tend to be increasingly broad-banded as the maximization of input entropy rate $\tilde{H}_W$ starts to receive priority. However, the predominant input energy remains concentrated at the first natural frequency of the system. Case 4 in Figure 3(a) represents the result when the maximization of input entropy rate $\tilde{H}_W$ is the dominant objective criterion. In this case, the critical input is highly broad-banded. In fact, the exact analytical solution of the input in this case is a band-limited noise, as discussed above. The maximum entropy rate for this case can be calculated analytically. The maximum entropy rate $\tilde{H}_W$ calculated by the numerical method matches with the analytical result approximately within 95% accuracy for the various GA runs. Thus, the result obtained using MGA defining the two endpoints of the trade-off curve in Figure 3(b) is validated.

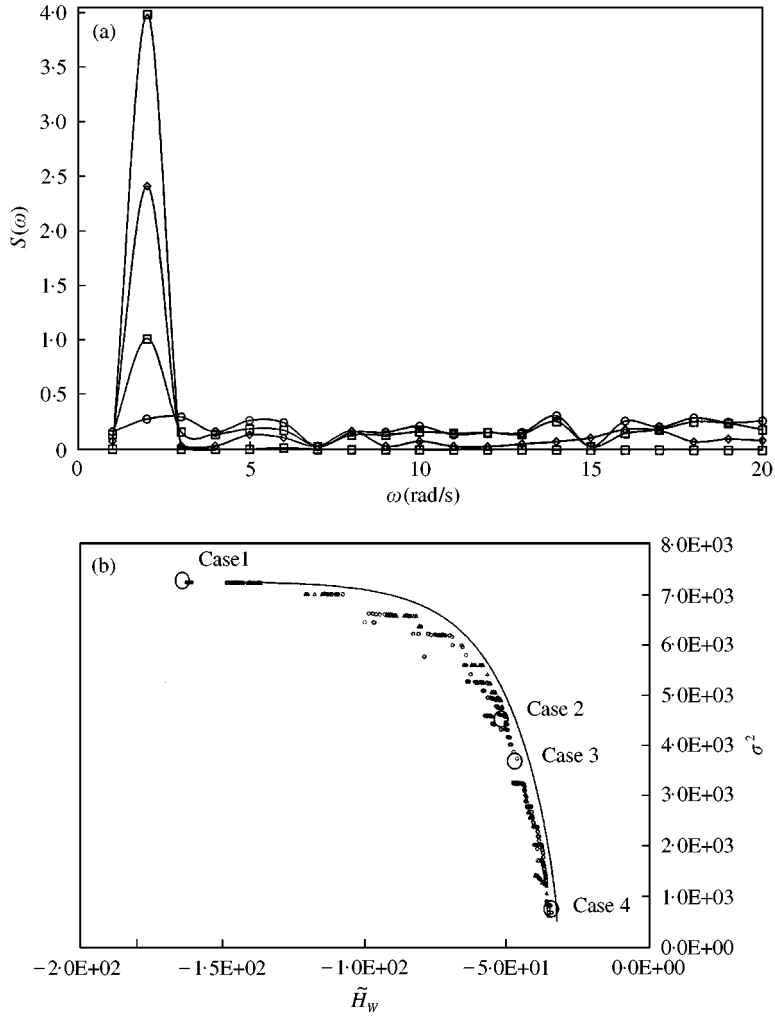


Figure 3. (a) The critical input PSD functions: □, cases 1 and 3; ◇, case 2; ○, case 4. (b) Trade-off curve of the response variance and input entropy rate: ——, check; ○, run 1; △, run 2; ○, run 3.

From the experience gathered from the numerical experiment, it is conjectured that the trade-off curve in this specific case of Figure 3(b) may be obtained simply by assigning the dominant input energy at the first natural frequency of the system and distributing the remaining energy equally in all the other frequencies in the band-limit of the excitation spectrum. This curve is also shown in Figure 3(b) termed as "check". A similar result is also obtained in references [9, 10] using calculus of variation when the non-preference optimization method is utilized. It can be easily observed that this plot envelopes the result obtained by the numerical method, serving again as the validation of the computer code. Thus, Figure 3 acts as a validation of the numerical program against the results obtained by other methods.

Figure 4(a) and (b) show the critical input PSD functions; and the trade-off curve of the mean response zero-crossing rate and the entropy rate of the excitation. In Figure 4(a), cases 1–5 show the critical input PSD functions for various levels of input entropy rate $\tilde{H}_W$. These inputs, in other words, represent the critical excitations which maximize the input

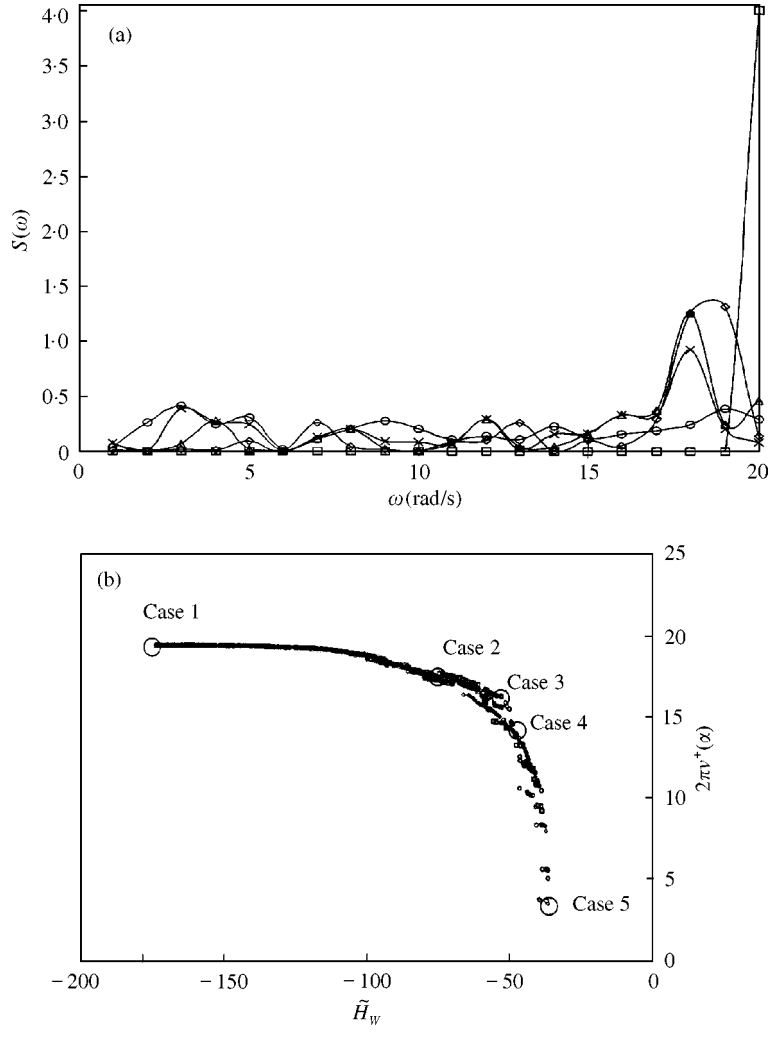


Figure 4. (a) The critical input PSD functions: □, cases 1; ◇, case 2; △, case; ×, case 4; ○, case 5. (b) The trade-off curve of the mean zero crossing rate versus input entropy rate ($\alpha = 0$): ◇, run 1; □, run 2; ○, runs 3 and 4.

entropy rate for various levels of the mean response zero crossing rate. Again, case 1 in Figure 4(a) shows the critical input entropy rate when the maximization of the mean response zero-crossing rate $\nu(0)$ is given the priority. Note again that the critical input is a highly narrow-banded signal with primary energy at the highest frequency in the excitation band-width for this specific case. This may be explained by the fact that the excitation with the dominant energy content at the highest frequency results in the maximum velocity response variance, but minimum displacement response variance in equation (7). Consequently, this input maximizes the mean response zero-crossing rate. Next, when the trade-off between the maximization of the input entropy rate and the mean response zero-crossing rate is considered, the critical input PSD functions are shown in cases 2–5, for increasing levels of input entropy rate. It can be observed from Figure 4(a) that the critical inputs tend to be increasingly broad-banded. However, the predominant energy in the critical inputs now shifts at the last natural frequency of the system for a moderate level of entropy rate (cases 2–4). Although the primary energy is concentrated at

the last natural frequency of the system, the rest of the input energy is now unevenly distributed on the remaining input frequency band limit, perhaps with a bias to the other natural frequencies of the system. The uneven energy distribution may also indicate the effect of strong non-linearity in both the objective functions. When the maximization of input entropy rate is given the priority, the critical input again becomes highly broad-banded tending towards a band-limited white noise, as expected.

## 4. CONCLUSIONS

A novel numerical scheme is developed to generate the trade-off curve of the maximum system response versus the maximum disorder in the input when the random excitation driving the linear system is partially specified. The approach makes use of Pareto optimization theory to deal with the conflicting requirement of system response maximization and the disorder in the input excitation. The numerical implementation is performed using a Multi-criteria Genetic Algorithm scheme to generate the trade-off curve.

In this paper, the primary emphasis is placed on the development of the numerical method. Only simple examples using a linear system are chosen to illustrate the method. In this study, the uncertainty is considered only in the specification of the input. However, the uncertainty in the system parameters is not accounted for. However, the uncertainty in the system parameters can also be important in many practical cases.

Additional studies are needed to extend the aforementioned analysis to incorporate the system uncertainty in addition to the uncertainty in the inputs. Furthermore, the method can be extended to the response of weakly non-linear systems using non-linear spectral analysis methods using Volterra series or the Weiner Hermite expansion approach.

From the point of view of reliability analysis, a structural system may consist of several elements each having multiple limit states. Consequently, a system can be configured as simple as a series system where the components are connected in series; a parallel system where the components are connected in parallel; a series–parallel or parallel–series system where some components are connected in series and the others are in parallel or *vice versa* leading to a complex network of configurations. It should be noted that only a single limit state is considered for the failure analysis in this paper. Consequently, it will be of interest to study the reliability of the linear parallel, series or combined systems due to an incompletely specified Gaussian load process. On the other hand, the method has to be extended to the case when the excitations to the systems are modelled as multi-dimensional Gaussian vector processes. All these aforementioned aspects require further investigation. Presently, some of these aspects are being investigated by the authors and will be published subsequently.

## REFERENCES

1. D. W. Tufts and D. A. Shnidman 1964 *Proceedings of IEEE* **52**, 1002–1007. Optimum waveforms subject to both energy and peak values constraints.
2. A. Papoulis 1967 *Proceedings of IEEE* **55**, 1677–1686. Limits on bandlimited signals.
3. A. Papoulis 1970 *IEEE Transactions on Circuit Theory* **ct-17**, 175–182. Maximum response with input energy constraints and the matched filter principle.
4. R. F. Drenick 1970 *Journal of Engineering Mechanics* **96**, 483–493. Model-free design of aseismic structures.
5. R. F. Drenick 1973 *Journal of Engineering Mechanics* **99**, 647–667. Aseismic design by way of critical excitations.
6. R. F. Drenick and C. B. Yun 1979 *Journal of Engineering Mechanics* **105**, 1879–1891. Reliability of seismic resistance predictions.

7. R. N. IYENGAR and C. S. MANOHAR 1985 *Paper MI* 5/6, *in Proceedings of the Eighth International Conference SmiRT*, *Brussels*. System dependent critical stochastic seismic excitations.
8. R. N. IYENGAR and C. S. MANOHAR 1987 *Journal of Engineering Mechanics* **113**, 529–541. Nonstationary random critical seismic excitations.
9. A. SARKAR 1995 *M.Sc. Thesis*, *Department of Civil Engineering*, *Indian Institute of Science*, Bangalore. Critical stochastic seismic excitation models for engineering structures.
10. C. S. MANOHAR and A. SARKAR 1995 *Earthquake Engineering and Structural Dynamics* **24**, 1549–1566. Critical earthquake input power spectral density function models for engineering structures.
11. A. PAPOULIS 1991 *Probability*, *Random Variable and Stochastic Processes*. New York: McGraw-Hill.
12. J. N. KAPUR 1993 *Maximum Entropy Models in Science and Engineering*. New Delhi: Wiley Eastern.
13. Y. K. LIN 1976 *Probabilistic Theory of Structural Dynamics*. New York: McGraw-Hill. Reprint R. E. Krieger, Melbourne, FL.
14. V. PARETO 1896–1897 *Cours d'Economic Politique*, Vols. 1 and 2, Rouge, Lausanne.
15. J. KOSKI 1981 *Proceedings of the* 11*th ONR Naval Structural Mechanics Symposium on Optimum Structural Design*, *University of Arizona*, *Tucson*, *AZ*. Multi-criterion Optimization in Structural Design.
16. D. E. GOLDBERG 1989 *Genetic Algorithms in Search*, *Optimization and Machine Learning*. Reading, MA: Addison-Wesley Publishing Company, Inc.